Micro-RNA networks in T-cell prolymphocytic leukemia reflect T-cell activation and shape DNA damage response and survival pathways

Till Braun,[1*] Markus Glaß,[2*] Linus Wahnschaffe,[1*] Moritz Otte,[1] Petra Mayer,[1] Marek Franitza,[3] Janine Altmüller,[3] Michael Hallek,[1] Stefan Hüttelmaier,[2#] Alexandra Schrader,[1#] and Marco Herling[1#]

[1]Department I of Internal Medicine, Center for Integrated Oncology (CIO), Aachen-Bonn-Cologne-Duesseldorf, Excellence Cluster for Cellular Stress Response and Aging-Associated Diseases (CECAD), Center for Molecular Medicine Cologne (CMMC), University of Cologne (UoC), Cologne; [2]Institute of Molecular Medicine, Section for Molecular Cell Biology, Faculty of Medicine, Martin Luther University Halle-Wittenberg, Charles Tanford Protein Center, Halle, and [3]Cologne Center for Genomics, Center for Molecular Medicine Cologne (CMMC), University of Cologne, Cologne, Germany

**TB, MG and LW contributed equally as co-first authors.*

#SH, AS and MH contributed equally as co-senior authors.

 doi:10.3324/haematol.2020.267500

Received: July 20, 2020.

Accepted: November 6, 2020.

Pre-published: November 19, 2020.

Correspondence: *MARCO HERLING* - Marco.Herling@medizin.uni-leipzig.de

Supplementary Methods

Age-matched healthy-donor derived controls

$CD3^+$ pan-T-cells of 6 age-matched healthy donors were used as controls (age older than 55 years). For that peripheral-blood mononuclear cells (PBMCs) were isolated from buffy coats by density gradient centrifugation (Histopaque, Sigma-Aldrich, St. Louis, Missouri, USA). Enrichment of $CD3^+$ T-cells was performed by negative selection from PBMCs using magnetic-bead based cell enrichment (Biolegend, San Diego, California, USA) according to manufacturer's guidelines. In order to compare T-PLL cells to TCR activated T-cells, PBMCs of 4 healthy donors were stimulated using CD3/CD28 antibody mediated cross-linking (OKT3, Biolegend; 15E8, Biolegend) and kept in culture for 72 hours. As unstimulated controls, PBMCs of the same donor were kept in culture as well. After 72 hours, $CD3^+$ T cells were enriched via negative magnetic selection (TCR-activated condition and unstimulated controls).

Total RNA isolation and library preparation

Total RNA was isolated from PBMCs of 46 T-PLL patients and $CD3^+$ pan-T-cells of 6 age-matched healthy controls using the mirVana kit (Thermofisher, Waltham, Massachusetts, USA) according to manufacturer's guidelines (total RNA isolation, no enrichment for small RNAs). In order to remove remaining DNA, DNAse treatment of samples was performed by using the DNA-free kit (Invitrogen, Carlsbad, California, USA). RNA quality was assessed using the 4150 TapeStation (Agilent, Santa Clara, California, USA) and samples with RNA integrity number (RIN) < 6 were excluded (median RIN=8.76). For polyA-RNA sequencing, samples were subjected to library preparation using the TruSeq® Stranded mRNA Library Prep kit (Illumina, San Diego, California, USA) and then sequenced on the NovaSeq 6000 platform (Illumina, San Diego, California, USA) according to standard protocols. For small RNA sequencing, library preparation was performed using the Small RNA-Seq Library Prep Kit (Lexogen, Vienna, Austria) including size selection with Lexogen's Gel extraction module. The barcoded libraries were size restricted between 140 and 170 bp. Samples were then analyzed using the HiSeq4000 platform (Illumina, San Diego, California, USA) according to manufacturer's instructions. Prior to sequencing, quality of both small RNA and polyA-RNA libraries was accessed using the 4150 TapeStation (Agilent, Santa Clara, California, USA) according to standard protocols.

Small RNA sequencing data processing and analysis

Low-quality read ends as well as remaining parts of sequencing adapters were clipped off using Cutadapt (v1.14). Trimmed reads were aligned to the human genome (UCSC hg38) using Bowtie2 (v2.3.2).[1] Indexing and sorting of mapped reads was performed using

samtools (v1.5).[2] FeatureCounts (v1.5.3)[3] was used for summarizing gene-mapped reads. MiRBase annotations (v22/GRCh 38) [4] were used for assigning mapped reads to known miR genes. Differential gene expression (DGE) was determined using R/edgeR (v3.26.8) [5] and applying Trimmed Mean of M-values (TMM) normalization. Counts Per Million (CPM) transformation was applied to obtain normalized expression values. Hierarchical clustering was performed by using Euclidean distances and Ward's clustering algorithm.[6] Separation of the samples into two clusters was conducted by cutting the clustering tree at the highest level (i.e. visual inspection).

PolyA-RNA sequencing data processing and analysis

Reads were aligned to the human genome (UCSC hg38) using Hisat2 (v2.1.0).[7] Indexing and sorting of mapped reads as well as removal of secondary alignments was performed using samtools (v1.5).[2] FeatureCounts (v1.5.3)[3] was used for summarizing gene-mapped reads. Ensembl annotations (GRCh 38.89) were used for assigning mapped reads to known genes. DGE was determined using R/edgeR (v3.26.8)[5] and applying TMM normalization. Fragments Per Kilobase of Million mapped reads (FPKM) transformation was applied to obtain normalized expression values. Hierarchical clustering was performed by using Euclidean distances and Ward's clustering algorithm.[6]

Quantitative real-time PCR

Isolated RNA from PBMCs of T-PLL patients (*n*=11) and $CD3^+$ pan-T-cells of age-matched healthy donors (*n*=4) was reverse-transcribed into cDNA using the TaqMan™ Advanced miRNA cDNA synthesis kit (Thermofisher, Waltham, Massachusetts, USA). TaqMan™ Advanced miRNA Assays for miR-223-3p, miR-141-3p, miR-200c-3p, and miR-30c-5p (Thermofisher, Waltham, Massachusetts, USA) were used for quantitative real-time PCRs according to the manufactures' instructions. Thermal cycling and detection were carried out using an ABI 7500 Fast System. MiR-30c-5p presented one of the lowest coefficients of variation among all samples (coefficient of variation=0.27, FC=1.06), accompanied by a low fold-change comparing T-PLL cases to normal T-cell controls. We, therefore, used miR-30c-5p as the endogenous control. Relative quantification was calculated by using the $2^{-\Delta\Delta CT}$ method, with the mean $2^{-\Delta\Delta CT}$ of the 4 healthy-donor derived samples as the reference for relative expression.

Clinical data analysis

Detailed information on clinical characteristics, cytogenetics, immunophenotypes, and follow up was accessed for all patients. To detect possible associations between these data and miR expression in 46 T-PLL patients, we performed a screening approach testing for an extended set of parameters. For miR-223-3p, miR-21, miR-29, and miR-200c/141, patients

were divided in groups using either the tertiles or the mean as cutoffs according to the distribution of expression values within the patient cohort. We *(i)* assigned T-PLL patients to a group according to the expression of the respective miR and *(ii)* then compared clinical data between these groups. As clinical data had a few blanks for some parameters in individual T-PLL patients, group sizes slightly differed between analyses of different miRs and parameters. Systematic comparison was then performed using Mann-Whitney-Wilcoxon (MWW) test and Fisher's exact test for continuous and categorial data, respectively. Associations of miR expression with overall survival (OS) from diagnosis were examined with log-rank statistics. Blood counts and clinical chemistry indices were evaluated at the time of sampling. All statistical analyses were carried out using the R software and R packages. A p-value < 0.05 was considered statistically significant.

References

1. Langmead B, Salzberg SL. Fast gapped-read alignment with Bowtie 2. Nat Methods. 2012;9(4):357–359.
2. Li H, Handsaker B, Wysoker A, et al. The Sequence Alignment/Map format and SAMtools. Bioinformatics. 2009;25(16):2078–2079.
3. Liao Y, Smyth GK, Shi W. featureCounts: an efficient general purpose program for assigning sequence reads to genomic features. Bioinformatics. 2013;30(7):923–930.
4. Kozomara A, Griffiths-Jones S. miRBase: annotating high confidence microRNAs using deep sequencing data. Nucleic Acids Res. 2013;42(D1):D68–D73.
5. Robinson MD, McCarthy DJ, Smyth GK. edgeR: a Bioconductor package for differential expression analysis of digital gene expression data. Bioinformatics. 2009;26(1):139–140.
6. Ward JH. Hierarchical Grouping to Optimize an Objective Function. J Am Stat Assoc. 1963;58(301):236–244.
7. Kim D, Langmead B, Salzberg SL. HISAT: a fast spliced aligner with low memory requirements. Nat Methods. 2015;12(4):357–360.

Figure S1: Primary T-PLL samples submitted to miR-ome sequencing exhibit tumor cell purities higher than 88%.

Bar chart displaying immunophenotypic data showing the proportion of $CD3^+$ cells in samples submitted to RNA sequencing. While T-PLL samples were sequenced out of total peripheral blood mononuclear cells (PBMCs, median purity 95.4%; range 88-99%), samples from age-matched healthy donors were enriched for $CD3^+$ T-cells by negative selection (median purity 90.2%; range 77-97%; see Methods section for details on cell isolation).

Figure S2: CPM values obtained by small-RNA sequencing indicate high absolute expression of significantly deregulated miRs in T-PLL.

Data supplement to Figure 1. Bar chart displaying mean CPM values for a total of 2094 miRs detected by small-RNA sequencing in at least one T-PLL patient (n=46 total cohort). MiRs which were significantly deregulated in 46-T-PLL cases compared to $CD3^+$ pan-T-cells of 6 healthy donors are highlighted in red (n=34), miRs not differentially expressed in T-PLL are displayed in grey. MiR-141-3p (mean CPM=26562) and miR-21-5p (mean CPM=15526), both differentially expressed in T-PLL, were among the miRs with highest absolute CPM values.

Figure S3: Differential expression of miR-223-3p, miR-200c-3p, and miR-141-3p in T-PLL as analyzed by quantitative real-time PCR

a) and b) Relative expression of miR-223-3p and miR-200c-3p as analyzed by quantitative real-time PCR (qRT-PCR; n=8 T-PLL, n=4 controls). Relative expression was calculated using the $2^{-\Delta\Delta CT}$ method, with the mean $2^{-\Delta\Delta CT}$ values of the 4 controls used as the reference. MiR-223-3p showed significant upregulation in T-PLL (fc=9.40; p=0.04, Welch's test).

c) ΔCT values of miR-141-3p as analyzed by qRT-PCR (n=8 T-PLL, n=4 controls). MiR-141-3p showed no observed expression in $CD3^+$ pan-T-cells of age-matched healthy donors, therefore expression is presented as ΔCT values. NE = no expression.

d) Pearson's correlation comparing small-RNA sequencing data and qRT-PCR results of miR-223-3p (n=8 T-PLL, n=4 $CD3^+$ pan-T-cells). Relative expression was calculated using expression of miR-30c-5p as an internal housekeeper control and using the mean expression of the 4 healthy-donor T-cell samples as a biological reference. Results from the qRT-PCR and small-RNA sequencing experiments showed a highly significant correlation (r^2=0.84, p<0.0001, Pearson).

Figure S4: Global miR-ome profiles of T-PLL cases are not associated with distinct T-cell phenotypes.

a and b) PCA based on differentially expressed miRs in T-PLL cases (n=46) compared to healthy-donor derived $CD3^+$ pan-T-cells (*Online Supplementary Table S1*). CD45RA / CD45RO as well as CD4 / CD8 surface expression was detected in primary T-PLL cells via flow cytometry.

Figure S5: T-PLL cells show altered gene expression profiles compared to healthy-donor derived $CD3^+$ pan-T-cells.

Differentially expressed mRNAs (n=948 transcripts; *Online Supplementary Table S5*) were evaluated using transcriptome sequencing analysis of peripheral-blood derived primary T-PLL cells (n=48 cases) and healthy-donor derived $CD3^+$ pan-T-cells (n=6 donors, isolation via negative selection). a) Volcano plot highlighting differentially expressed mRNAs in blue (lower expression) and red (higher expression) colors. Given percentages indicate relative proportions based on all identified mRNAs (n=18215 totally detected transcripts).

b) PCA and c) heatmaps based on the 100 most differentially expressed mRNAs. Left heatmap: mean *Fragments Per Kilobase Million* (FPKM) values compared between healthy-donor derived controls (n=6) and T-PLL (n=48; red=higher expression; blue=lower expression). Right heatmap: Colors represent z-scores of respective FPKM values calculated for each mRNA (blue=lower z-score; red=higher z-score).

Figure S6: Primary $CD3^+$ pan-T-cells show elevated activation marker expression upon CD3/CD28 antibody mediated crosslinking.

Data supplementing Figure 2B and C) and *Online Supplementary Figure S7*: a) Primary $CD3^+$ T-cells were isolated from peripheral blood of healthy donors using PBMC isolation and subsequent MACS enrichment after 72 hrs. (negative selection, see Methods section for details). Sample purities were assessed using flow cytometry for $CD3^+$ positive cells within the isolates (median: 94.8%; range: 78-99%).

b) Stimulation control of TCR-activated healthy-donor derived T-cells (Figure 2B and C): isolated PBMCs were submitted to antibody-mediated CD3/CD28 cross-linking to induce TCR activation. Surface marker expression (CD25, CD38, CD69) was analyzed by flow cytometry at 72 hrs. after such TCR (CD3/CD28) stimulation.

c) Overlay plots of TCR-stimulated condition to unstimulated control (CD25, CD38, CD69 surface expression) of one exemplary healthy-donor sample.

Figure S7: TCR activation induces global changes in miR expression profiles of healthy-donor derived CD3$^+$ pan-T-cells.

Age-matched healthy-donor derived PBMCs were isolated via density gradient centrifugation. TCR-mediated T-cell activation was achieved via continued antibody-based CD3/CD28 cross-linking. After 72 hrs., CD3$^+$ primary human T-cells were isolated by MACS enrichment (negative selection; see Method section for details; cell purities are given in *Online Supplementary Figure S6A*, see *Online Supplementary Figure S6B and C* for control experiments). MiR-ome profiles were generated using small-RNA sequencing. a) Volcano plot showing log2 fc and –log10 FDR values of differentially expressed miRs in response to CD3/CD28 stimulation. Given percentages show relative proportions based on all identified miRs (n=56/1587 totally detected miRs; FDR<0.05).

b) PCA of differentially expressed miRNAs upon CD3/CD28 cross-linking (light green: unstimulated controls; dark green: stimulated condition).

c) Heatmap showing miR expression in unstimulated vs. stimulated healthy-donor derived T-cells (n=52 miRs; FDR<0.05). Colors represent z-scores of respective CPM values calculated for each miR (blue=lower z-score; red=higher z-score).

Figure S8: Functional associations of predicted miR-targets using GSEA highlight processes of DNA-damage responses and pro-survival signaling.

Data supplement Figure 3A: GSEA heatmap based on miR associated mRNAs. GSEAs were conducted for all significantly deregulated miRs (n=34 miRs; *Online Supplementary Table S1*) using ranked correlation indices between mRNA and miR expression in 41 T-PLL and 6 healthy-donor derived T-cell samples. Color code summarizes NES scores (blue=negative NES; red=positive NES). Statistical significance is summarized via asterisks (*p<0.05; **p<0.01; ***p<0.001; Kolmogorov-Smirnov-test).

Figure S9: Reduced expression of miR-21 is associated with alterations of apoptosis and cell-cycle regulators.

a) Differential expression of miR-21 family members as analyzed by small-RNA sequencing shows significant downregulation of miR-21-3p (fc=0.27 ; p<0.0001) and miR-21-5p (fc=0.31; p<0.0001, n=46 T-PLL cases, n=6 normal T-cell controls).

b) Exemplary GSEA plots of miR-21 correlated mRNAs: *APOPTOSIS: N*ES=3.89, q<0.0001 (miR-21-5p correlated mRNAs); *G2M_CHECKPOINT:* NES=2.39, q=0.001 (miR-21-3p correlated mRNAs).

c) Predicted targets (by seed sequences, see Methods section for details) correlating negatively with miR-21 expression in all analyzed cases and controls implicate regulatory networks involved in DNA-damage response and pro-survival signaling. Font color represents differential expression of mRNAs comparing T-PLL cells (n=48 cases) to healthy-donor derived $CD3^+$ pan-T-cells (n=6 donors; for description of global mRNA sequencing results refer to Figure 2A: blue=lower expression, red=higher expression). Color of highlighted boxes indicates assignment of genes to functional groups of DNA-damage response pathways (black) and pro-survival signaling (grey).

d) Low miR-21 expression was associated with higher white blood cell counts (WBC) (median: 154 vs. 90.0 G/l; p=0.02; MWW) and lower platelet counts (median: 110 vs. 153 G/l; p=0.03; MWW) at the time of sample acquisition. See *Online Supplementary Table S10* for summary of clinical data. Groups were divided by the mean miR-21 expression value.

e) Low miR-21 expression was associated with higher serum lactate dehydrogenase (LDH) levels at the time of sample acquisition (median: 933 vs. 522 U/l; p=0.02; MWW). Groups were divided by the mean miR-21 expression.

Figure S10: Reduced expression of miR-29 clusters is associated with alterations of cell survival signaling and cell-cycle regulators reflected in more activated phenotypes and a more aggressive disease course.

a) Differential expression of miR-29 family members as analyzed by small-RNA sequencing showed significant downregulation of miR-29a-3p (fc=0.29; p<0.0001), miR-29b-1-5p (fc=0.47; p=0.001), and miR-29c-3p (fc=0.29; p<0.0001) in 46 T-PLL, as compared to 6 normal T-cell control samples.

b) Exemplary GSEA plots of miR-29-correlated mRNAs: *E2F_TARGETS:* NES=-3.52, q<0.0001, *TNFA_SIGNALING_VIA_NFKB:* NES=-2.08, q=0.01 (both based on miR-29a-3p correlated mRNAs).

c) Predicted targets (by seed sequences, see Methods section for details) that negatively correlate with miR-29 expression in all analyzed cases and controls revealed regulatory networks involved in DNA-damage response pathways and pro-survival signaling. Font color represents differential expression of mRNAs comparing T-PLL cells (n=48 cases) and healthy-donor derived $CD3^+$ pan-T-cells (n=6 donors; for description of global mRNA sequencing results refer to Figure 2A and *Online Supplementary Table S5*, blue=lower expression; red=higher expression). Color of highlighted boxes represents assignment of genes to functional groups of DNA-damage response pathways (black) and pro-survival signaling (grey).

d) Groups of low and high miR-29 expression were assigned by results of small-RNA sequencing: Cases were divided into three tertiles and the lower was compared against the upper tertile. Groups were then evaluated for CD38 and CD69 surface expression using flow cytometry. T-PLL cases with low miR-29 expression levels presented with a more activated T-cell phenotype (median CD38 expression: 43.1% vs. 12.9%, p=0.02; median CD69 expression: 27.9% vs. 0.89%, p=0.02; MWW).
e and f) Platelet counts and serum LDH values of analyzed cases were assessed (see *Online Supplementary Table S11* for a summary of clinical data). Groups were divided into tertiles of miR-29 expression and the lower was compared against the upper tertile using MWW. e) Low miR-29 expression was associated with lower platelet counts at the time the sample was taken (median: 110 vs 186 G/l; p=0.15; MWW) and with f) higher serum LDH levels at the time of sample (median: 1850 vs 708 U/l; p=0.06; MWW).

Figure S11: Low miR-29 expression is associated with higher rates of effusions and more prevalent in cases with genomic *ATM* deletions.
Groups of low, medium, and high miR-29c-3p expression were assigned by results of small-RNA sequencing using tertile-based expression levels. Clinical presentation of cases was recorded for all analyzed T-PLL patients (see *Online Supplementary Table S11* for the comprehensive dataset) and the high expression group was compared against the low expression tertile. a) Cases with low miR-29c-3p expression showed a higher proportion of effusions (n=6/12 vs. n=1/10 cases; p=0.07; Fisher's exact test).
b) Genomic deletions of *ATM* were assessed using FISH studies probing the 11q22.3 consensus region. Cases with low miR-29b-1-5p expression showed a significantly higher proportion of *ATM* deletions (n=9/11 vs. n=1/11 cases; p=0.002; Fisher's exact test).

Figure S1

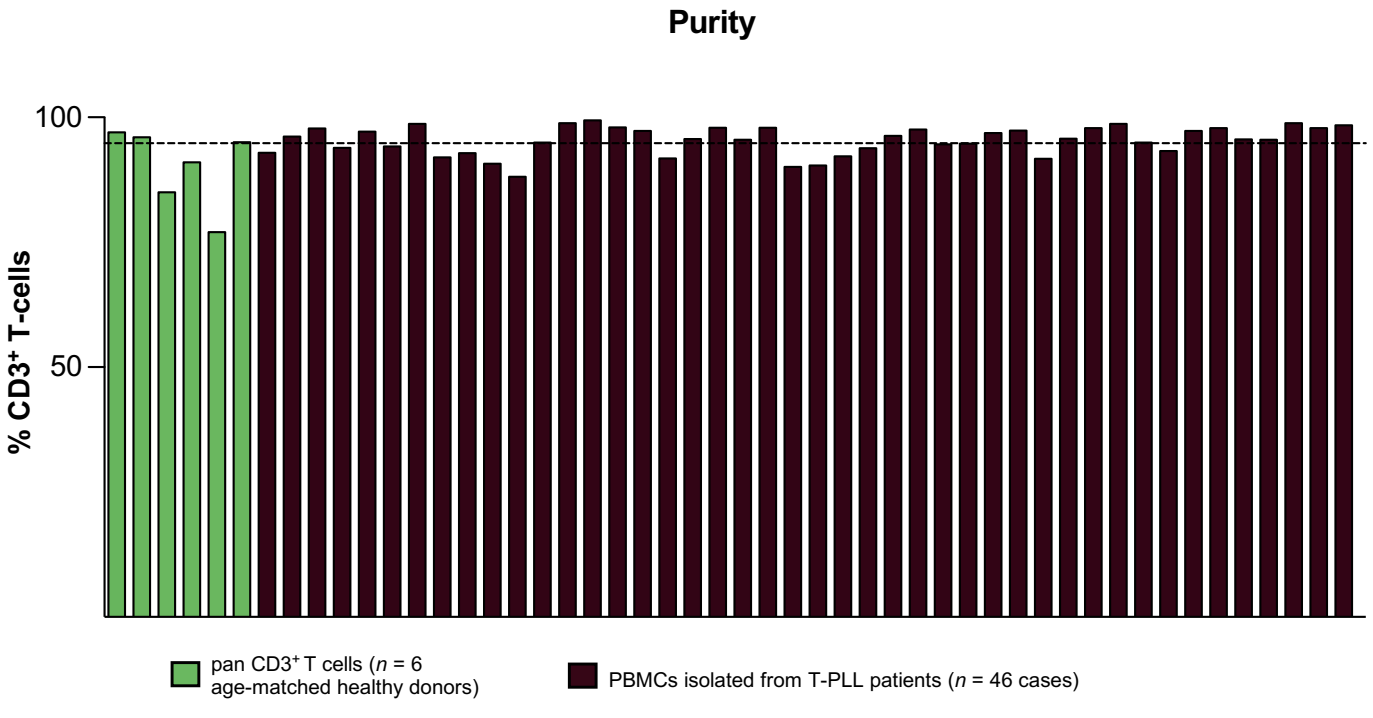
Purity
100
50
% CD3+ T-cells
pan CD3+ T cells (n = 6 age-matched healthy donors)
PBMCs isolated from T-PLL patients (n = 46 cases)

Figure S2

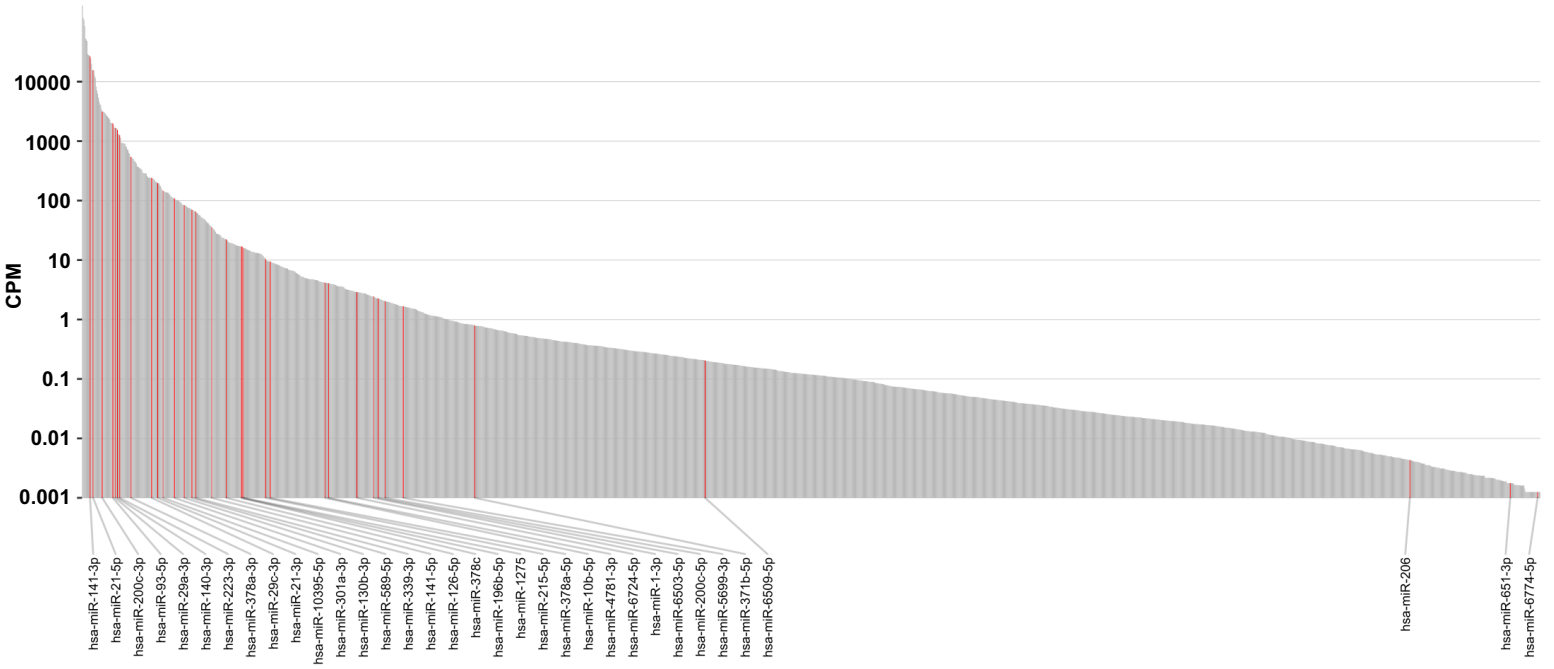
CPM
10000
1000
100
10
1
0.1
0.01
0.001
hsa-miR-141-3p
hsa-miR-21-5p
hsa-miR-200c-3p
hsa-miR-93-5p
hsa-miR-29a-3p
hsa-miR-140-3p
hsa-miR-223-3p
hsa-miR-378a-3p
hsa-miR-29c-3p
hsa-miR-21-3p
hsa-miR-10395-5p
hsa-miR-301a-3p
hsa-miR-130b-3p
hsa-miR-589-5p
hsa-miR-339-3p
hsa-miR-141-5p
hsa-miR-126-5p
hsa-miR-378c
hsa-miR-196b-5p
hsa-miR-1275
hsa-miR-215-5p
hsa-miR-378a-5p
hsa-miR-10b-5p
hsa-miR-4781-3p
hsa-miR-6724-5p
hsa-miR-1-3p
hsa-miR-6503-5p
hsa-miR-200c-5p
hsa-miR-5699-3p
hsa-miR-371b-5p
hsa-miR-6509-5p
hsa-miR-206
hsa-miR-651-3p
hsa-miR-6774-5p

Figure S3

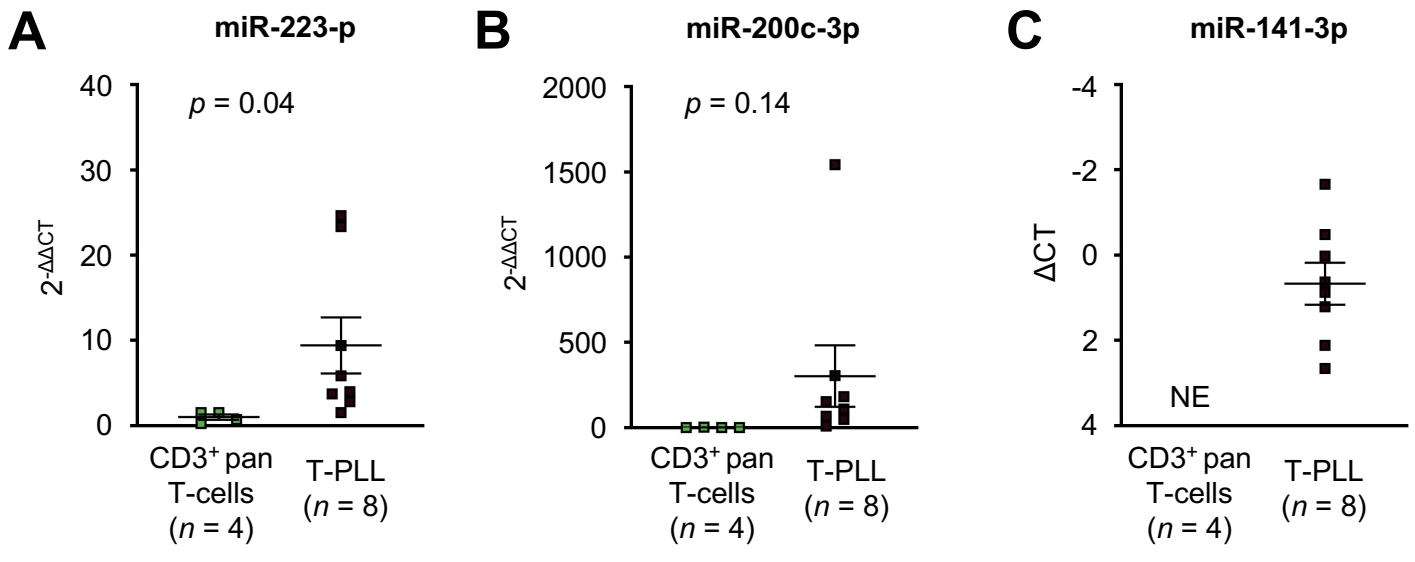
A
miR-223-p
p = 0.04
2-ΔΔCT
40
30
20
10
0
CD3+ pan T-cells (n = 4)
T-PLL (n = 8)
B
miR-200c-3p
p = 0.14
2-ΔΔCT
2000
1500
1000
500
0
CD3+ pan T-cells (n = 4)
T-PLL (n = 8)
C
miR-141-3p
ΔCT
-4
-2
0
2
4
NE
CD3+ pan T-cells (n = 4)
T-PLL (n = 8)

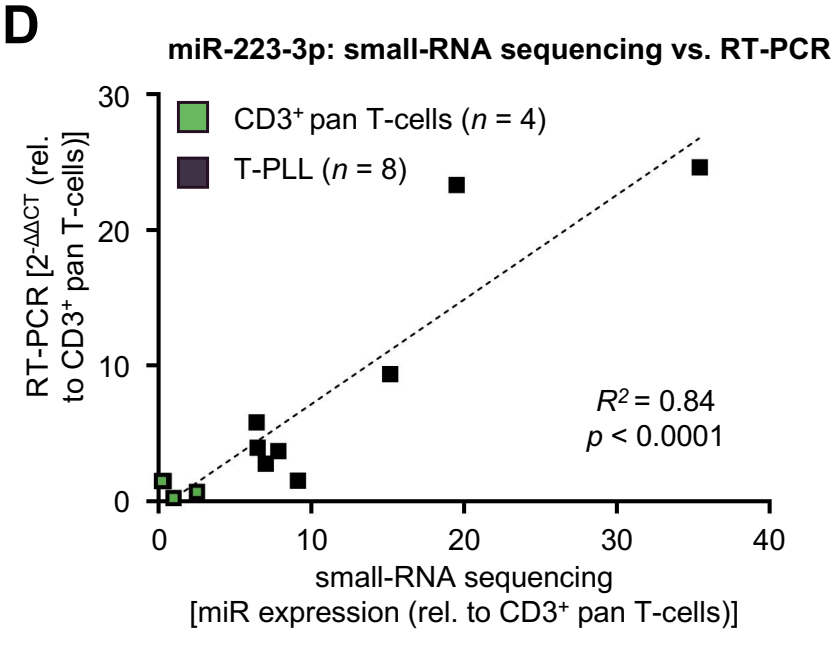
D
miR-223-3p: small-RNA sequencing vs. RT-PCR
CD3+ pan T-cells (n = 4)
T-PLL (n = 8)
RT-PCR [2-ΔΔCT (rel. to CD3+ pan T-cells)]
30
20
10
0
R2 = 0.84
p < 0.0001
0
10
20
30
40
small-RNA sequencing
[miR expression (rel. to CD3+ pan T-cells)]

Figure S4

A

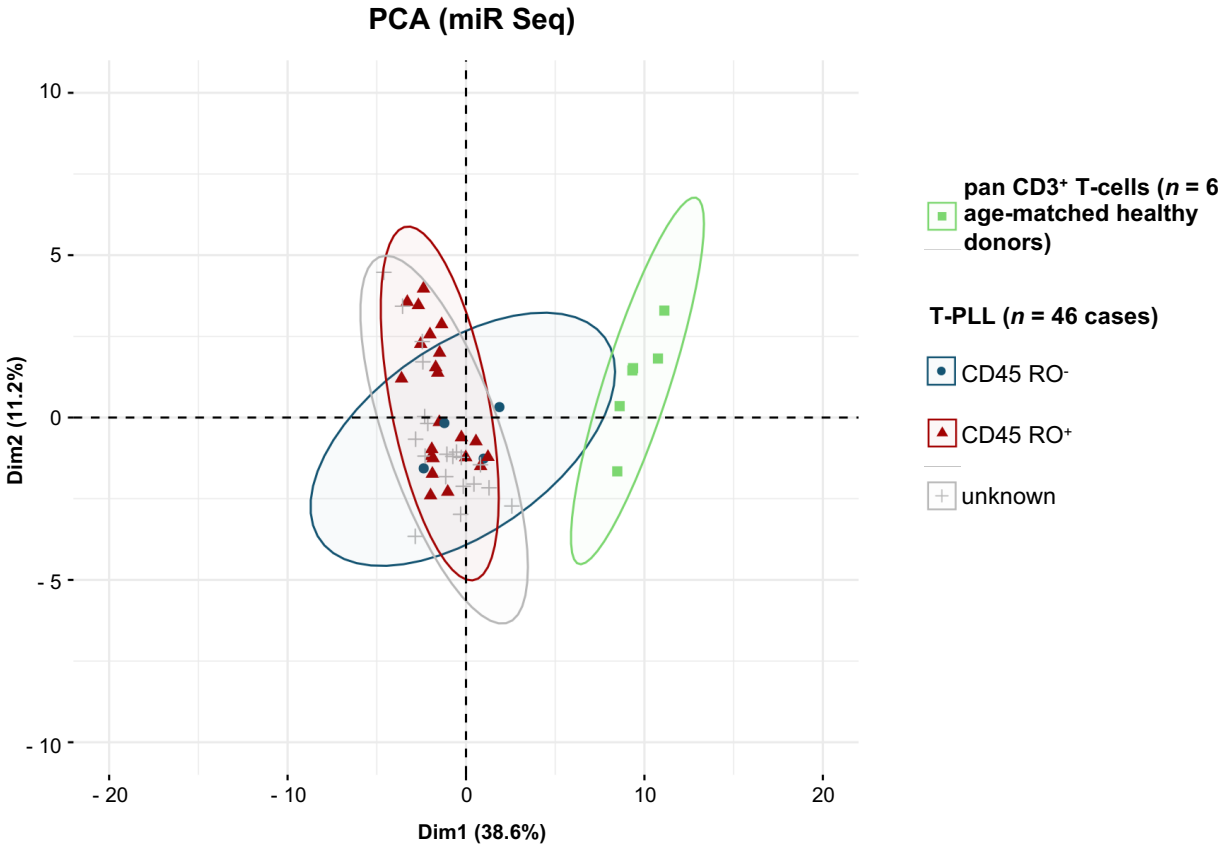
PCA (miR Seq)
Dim2 (11.2%)
Dim1 (38.6%)
10
5
0
- 5
- 10
- 20
- 10
0
10
20
pan CD3⁺ T-cells (n = 6 age-matched healthy donors)
T-PLL (n = 46 cases)
CD45 RO⁻
CD45 RO⁺
unknown

B

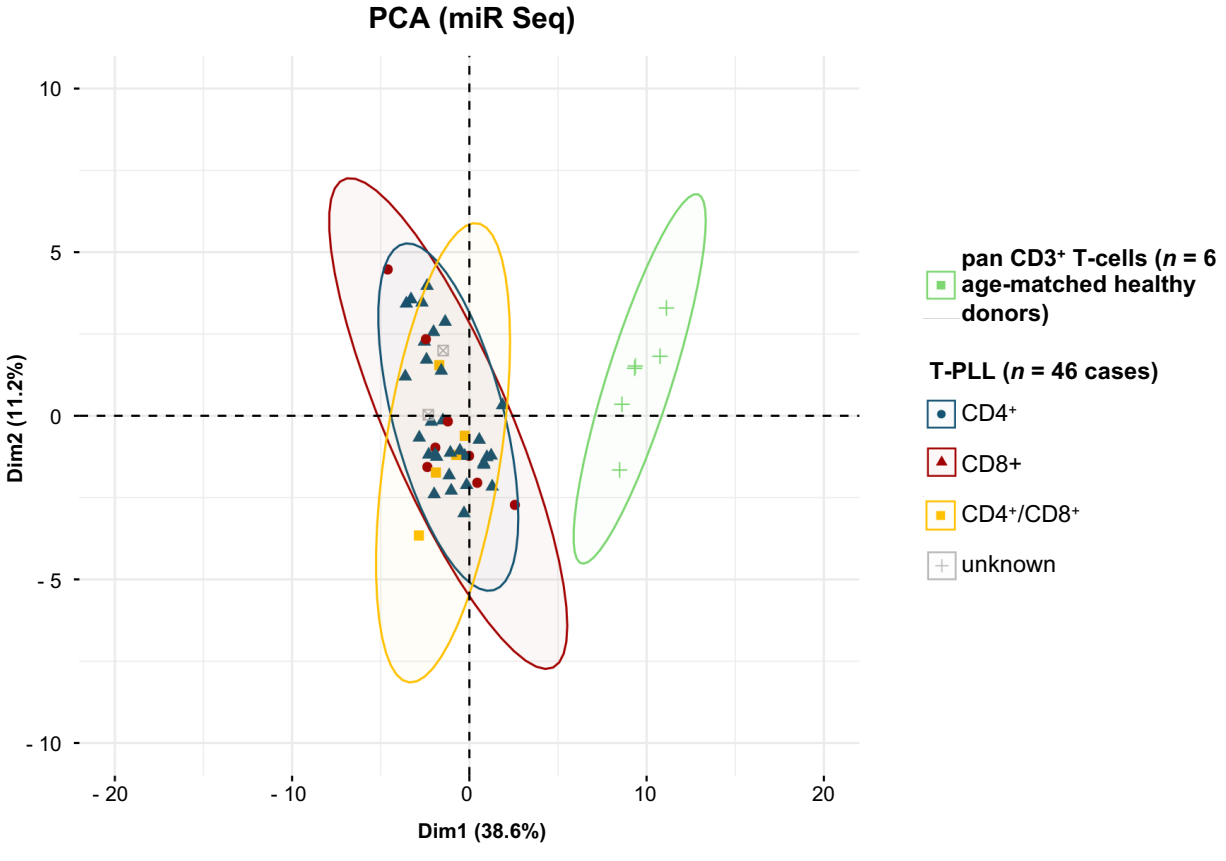
PCA (miR Seq)
Dim2 (11.2%)
Dim1 (38.6%)
10
5
0
- 5
- 10
- 20
- 10
0
10
20
pan CD3⁺ T-cells (n = 6 age-matched healthy donors)
T-PLL (n = 46 cases)
CD4⁺
CD8+
CD4⁺/CD8⁺
unknown

Figure S5

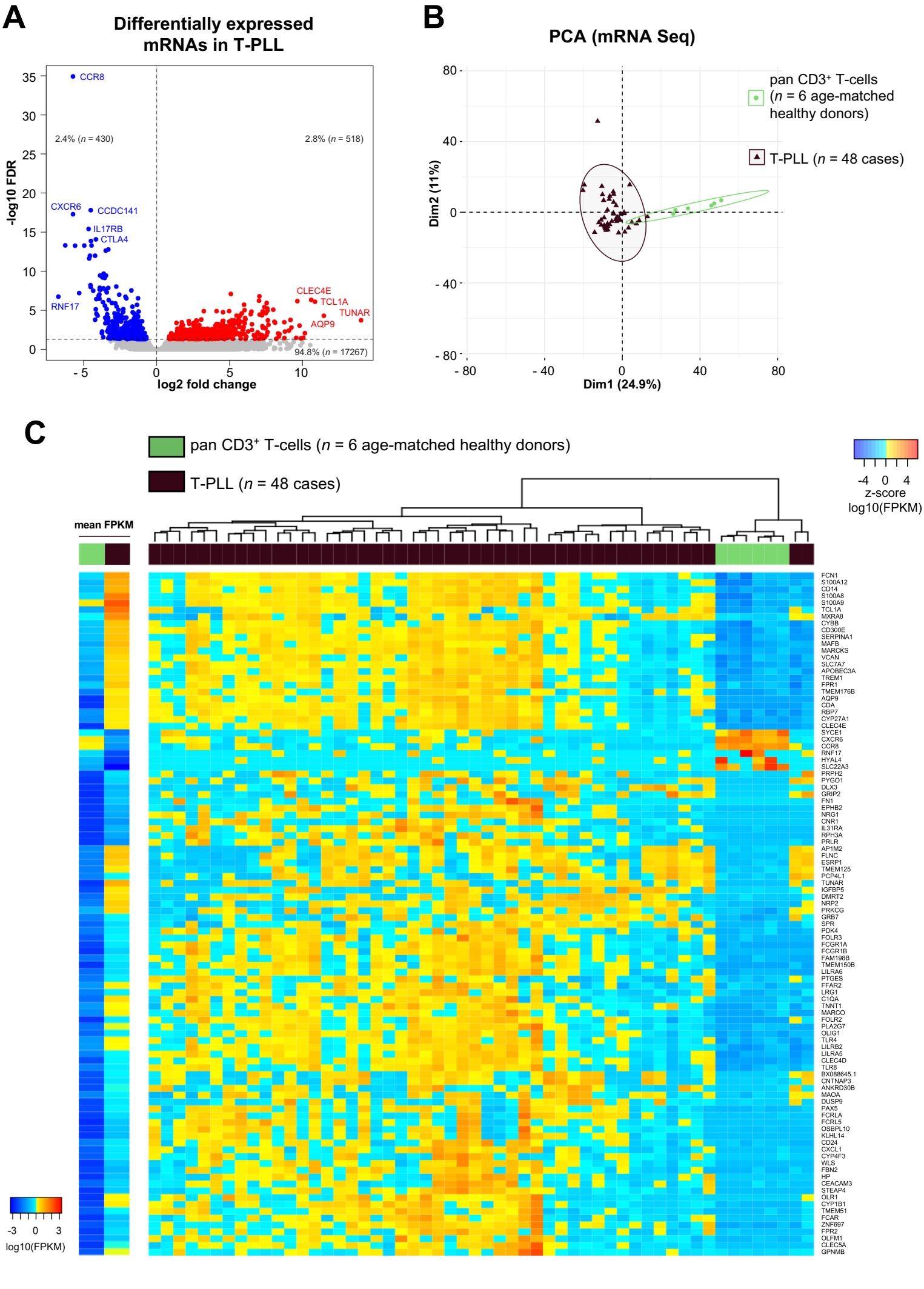
A
Differentially expressed mRNAs in T-PLL
-log10 FDR
log2 fold change
CCR8
CXCR6
CCDC141
IL17RB
CTLA4
RNF17
CLEC4E
TCL1A
TUNAR
AQP9
2.4% (n = 430)
2.8% (n = 518)
94.8% (n = 17267)
B
PCA (mRNA Seq)
pan CD3+ T-cells (n = 6 age-matched healthy donors)
T-PLL (n = 48 cases)
Dim1 (24.9%)
Dim2 (11%)
C
pan CD3+ T-cells (n = 6 age-matched healthy donors)
T-PLL (n = 48 cases)
mean FPKM
z-score log10(FPKM)
log10(FPKM)

Figure S6

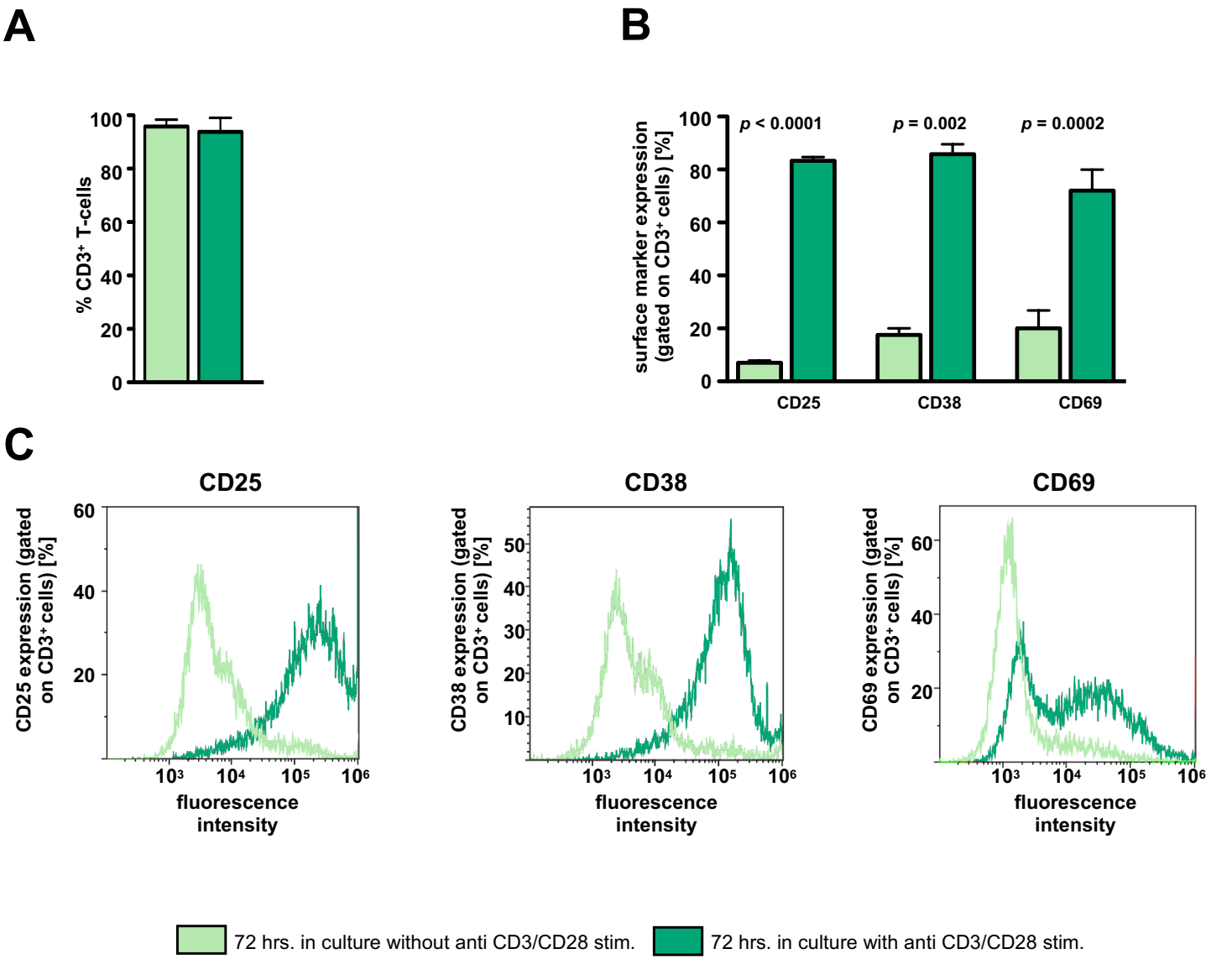
A
B
C
% CD3+ T-cells
surface marker expression (gated on CD3+ cells) [%]
p < 0.0001
p = 0.002
p = 0.0002
CD25
CD38
CD69
CD25 expression (gated on CD3+ cells) [%]
CD38 expression (gated on CD3+ cells) [%]
CD69 expression (gated on CD3+ cells) [%]
fluorescence intensity
72 hrs. in culture without anti CD3/CD28 stim.
72 hrs. in culture with anti CD3/CD28 stim.

Figure S7

A **Differentially expressed miRs upon anti-CD3/CD28 stimulation in pan T-cells derived from healthy controls**

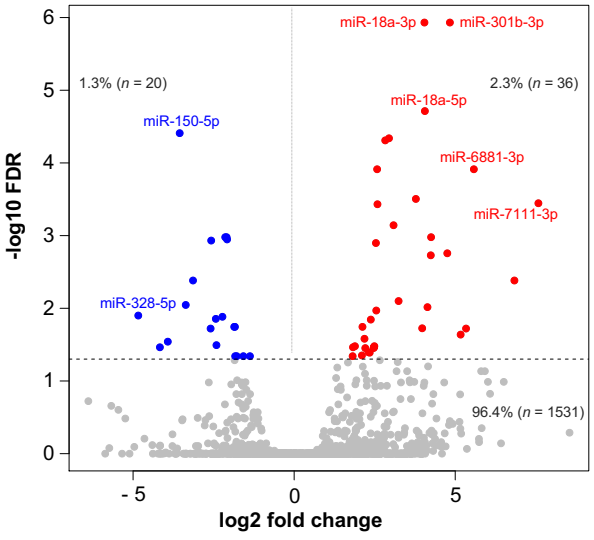

B

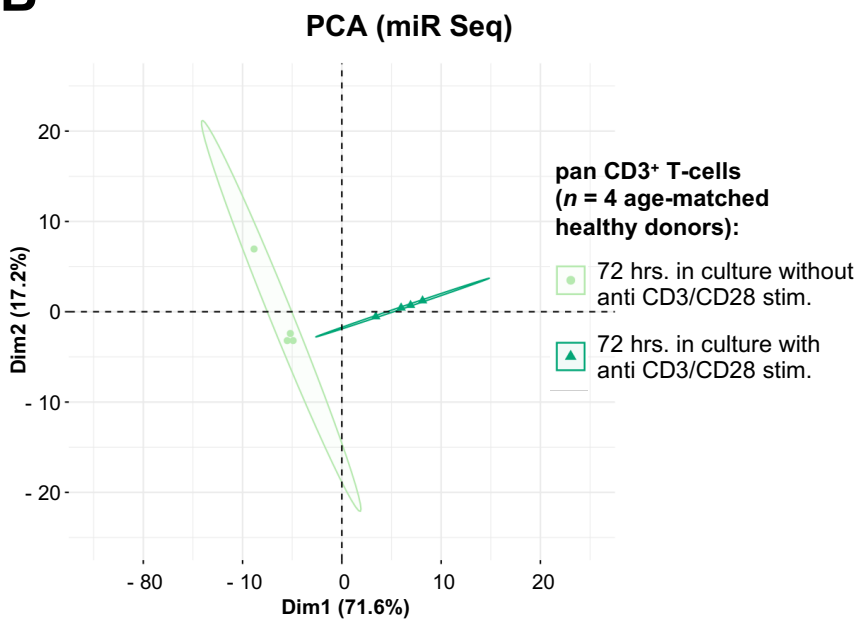

C

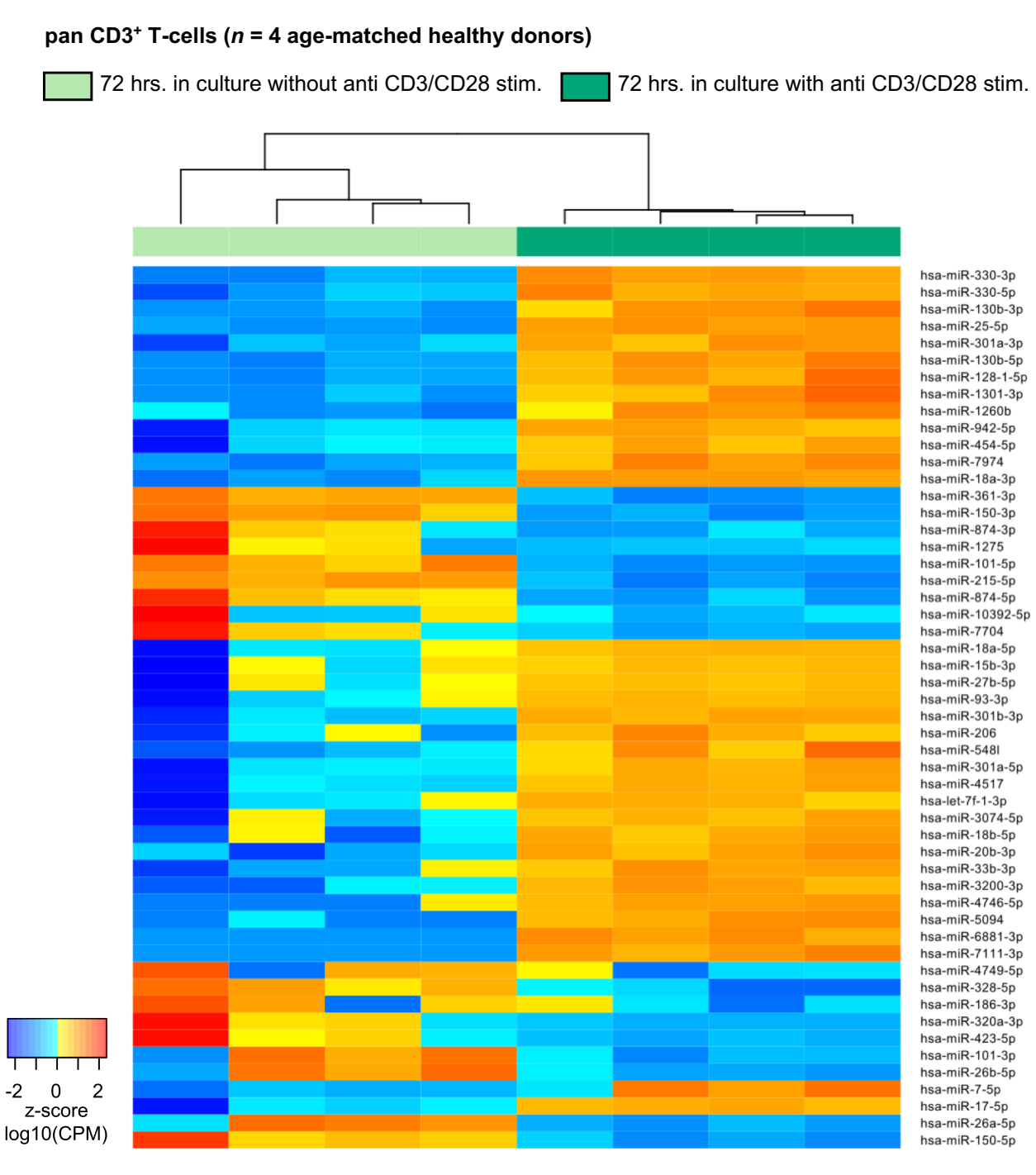

Figure S8

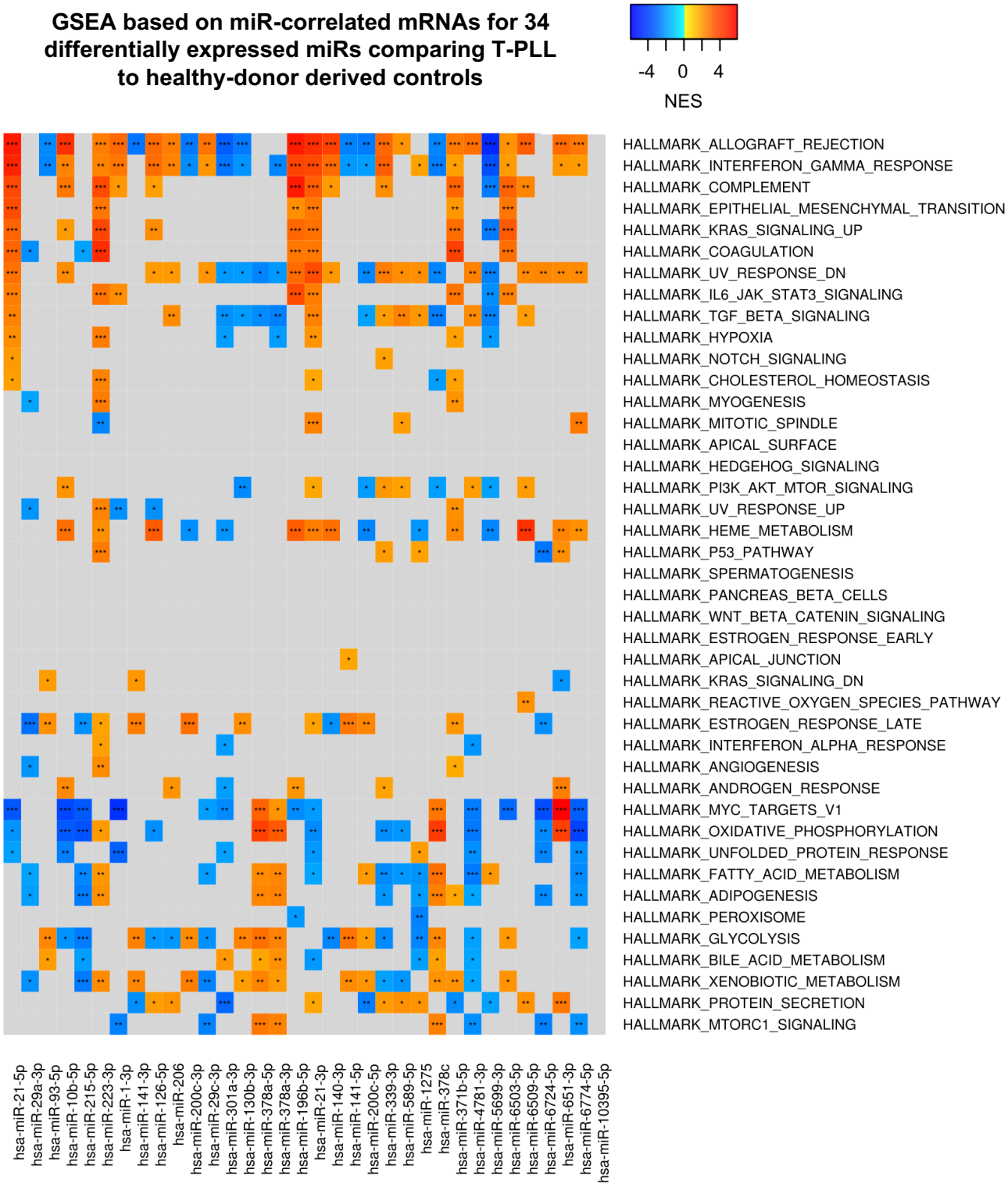
GSEA based on miR-correlated mRNAs for 34 differentially expressed miRs comparing T-PLL to healthy-donor derived controls
-4
0
4
NES
HALLMARK_ALLOGRAFT_REJECTION
HALLMARK_INTERFERON_GAMMA_RESPONSE
HALLMARK_COMPLEMENT
HALLMARK_EPITHELIAL_MESENCHYMAL_TRANSITION
HALLMARK_KRAS_SIGNALING_UP
HALLMARK_COAGULATION
HALLMARK_UV_RESPONSE_DN
HALLMARK_IL6_JAK_STAT3_SIGNALING
HALLMARK_TGF_BETA_SIGNALING
HALLMARK_HYPOXIA
HALLMARK_NOTCH_SIGNALING
HALLMARK_CHOLESTEROL_HOMEOSTASIS
HALLMARK_MYOGENESIS
HALLMARK_MITOTIC_SPINDLE
HALLMARK_APICAL_SURFACE
HALLMARK_HEDGEHOG_SIGNALING
HALLMARK_PI3K_AKT_MTOR_SIGNALING
HALLMARK_UV_RESPONSE_UP
HALLMARK_HEME_METABOLISM
HALLMARK_P53_PATHWAY
HALLMARK_SPERMATOGENESIS
HALLMARK_PANCREAS_BETA_CELLS
HALLMARK_WNT_BETA_CATENIN_SIGNALING
HALLMARK_ESTROGEN_RESPONSE_EARLY
HALLMARK_APICAL_JUNCTION
HALLMARK_KRAS_SIGNALING_DN
HALLMARK_REACTIVE_OXYGEN_SPECIES_PATHWAY
HALLMARK_ESTROGEN_RESPONSE_LATE
HALLMARK_INTERFERON_ALPHA_RESPONSE
HALLMARK_ANGIOGENESIS
HALLMARK_ANDROGEN_RESPONSE
HALLMARK_MYC_TARGETS_V1
HALLMARK_OXIDATIVE_PHOSPHORYLATION
HALLMARK_UNFOLDED_PROTEIN_RESPONSE
HALLMARK_FATTY_ACID_METABOLISM
HALLMARK_ADIPOGENESIS
HALLMARK_PEROXISOME
HALLMARK_GLYCOLYSIS
HALLMARK_BILE_ACID_METABOLISM
HALLMARK_XENOBIOTIC_METABOLISM
HALLMARK_PROTEIN_SECRETION
HALLMARK_MTORC1_SIGNALING
hsa-miR-21-5p
hsa-miR-29a-3p
hsa-miR-93-5p
hsa-miR-10b-5p
hsa-miR-215-5p
hsa-miR-223-3p
hsa-miR-1-3p
hsa-miR-141-3p
hsa-miR-126-5p
hsa-miR-206
hsa-miR-200c-3p
hsa-miR-29c-3p
hsa-miR-301a-3p
hsa-miR-130b-3p
hsa-miR-378a-5p
hsa-miR-378a-3p
hsa-miR-196b-5p
hsa-miR-21-3p
hsa-miR-140-3p
hsa-miR-141-5p
hsa-miR-200c-5p
hsa-miR-339-3p
hsa-miR-589-5p
hsa-miR-1275
hsa-miR-378c
hsa-miR-371b-5p
hsa-miR-4781-3p
hsa-miR-5699-3p
hsa-miR-6503-5p
hsa-miR-6509-5p
hsa-miR-6724-5p
hsa-miR-651-3p
hsa-miR-6774-5p
hsa-miR-10395-5p

Figure S9

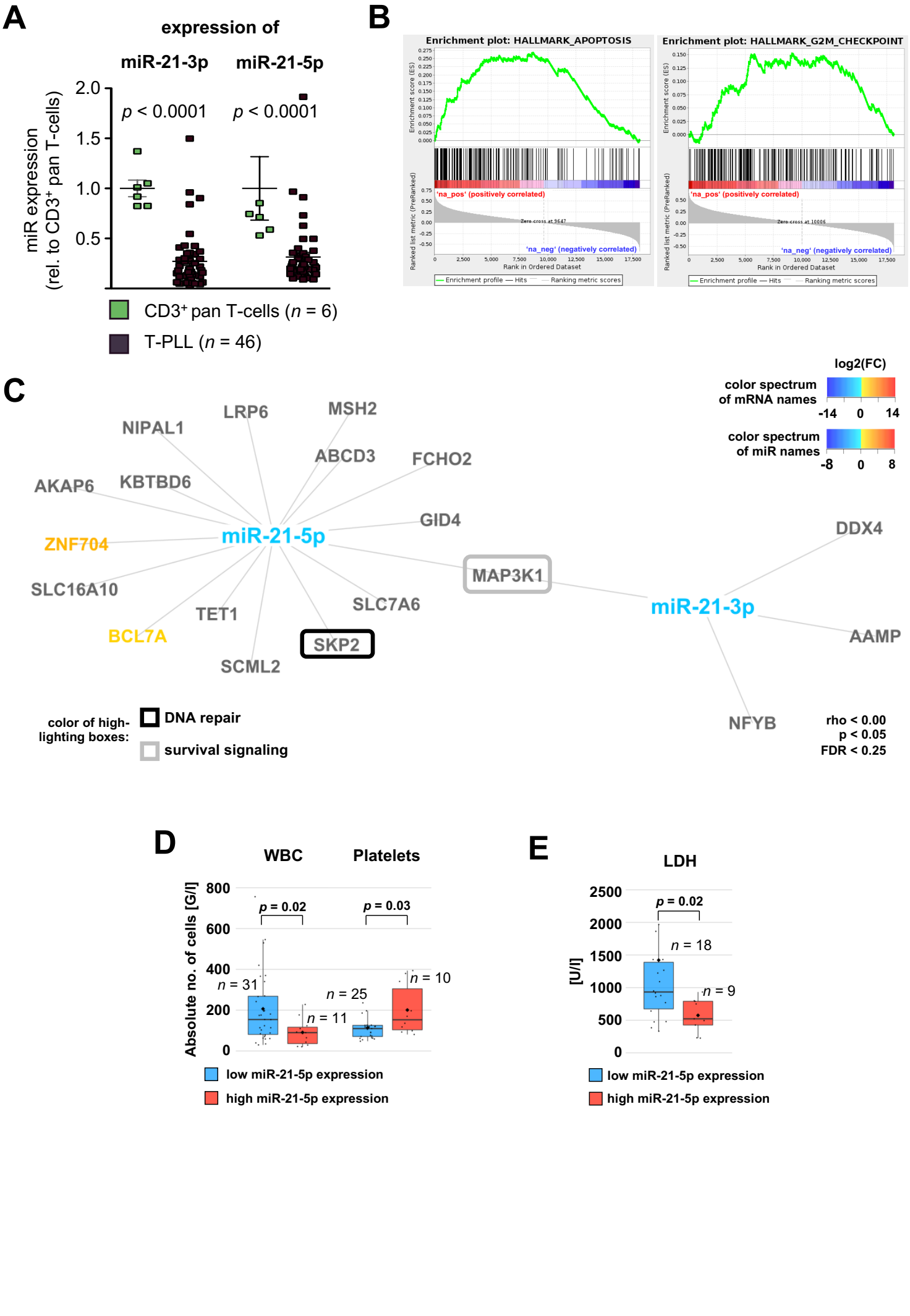
A
expression of
miR-21-3p
miR-21-5p
miR expression (rel. to CD3⁺ pan T-cells)
p < 0.0001
p < 0.0001
CD3⁺ pan T-cells (n = 6)
T-PLL (n = 46)
B
Enrichment plot: HALLMARK_APOPTOSIS
Enrichment plot: HALLMARK_G2M_CHECKPOINT
'na_pos' (positively correlated)
'na_neg' (negatively correlated)
Rank in Ordered Dataset
Enrichment profile
Hits
Ranking metric scores
C
log2(FC)
color spectrum of mRNA names
color spectrum of miR names
LRP6
MSH2
NIPAL1
ABCD3
FCHO2
AKAP6
KBTBD6
GID4
ZNF704
miR-21-5p
DDX4
MAP3K1
SLC16A10
SLC7A6
miR-21-3p
TET1
BCL7A
SKP2
AAMP
SCML2
NFYB
color of high-lighting boxes:
DNA repair
survival signaling
rho < 0.00
p < 0.05
FDR < 0.25
D
WBC
Platelets
Absolute no. of cells [G/l]
p = 0.02
p = 0.03
n = 31
n = 11
n = 25
n = 10
low miR-21-5p expression
high miR-21-5p expression
E
LDH
[U/l]
p = 0.02
n = 18
n = 9
low miR-21-5p expression
high miR-21-5p expression

Figure S10

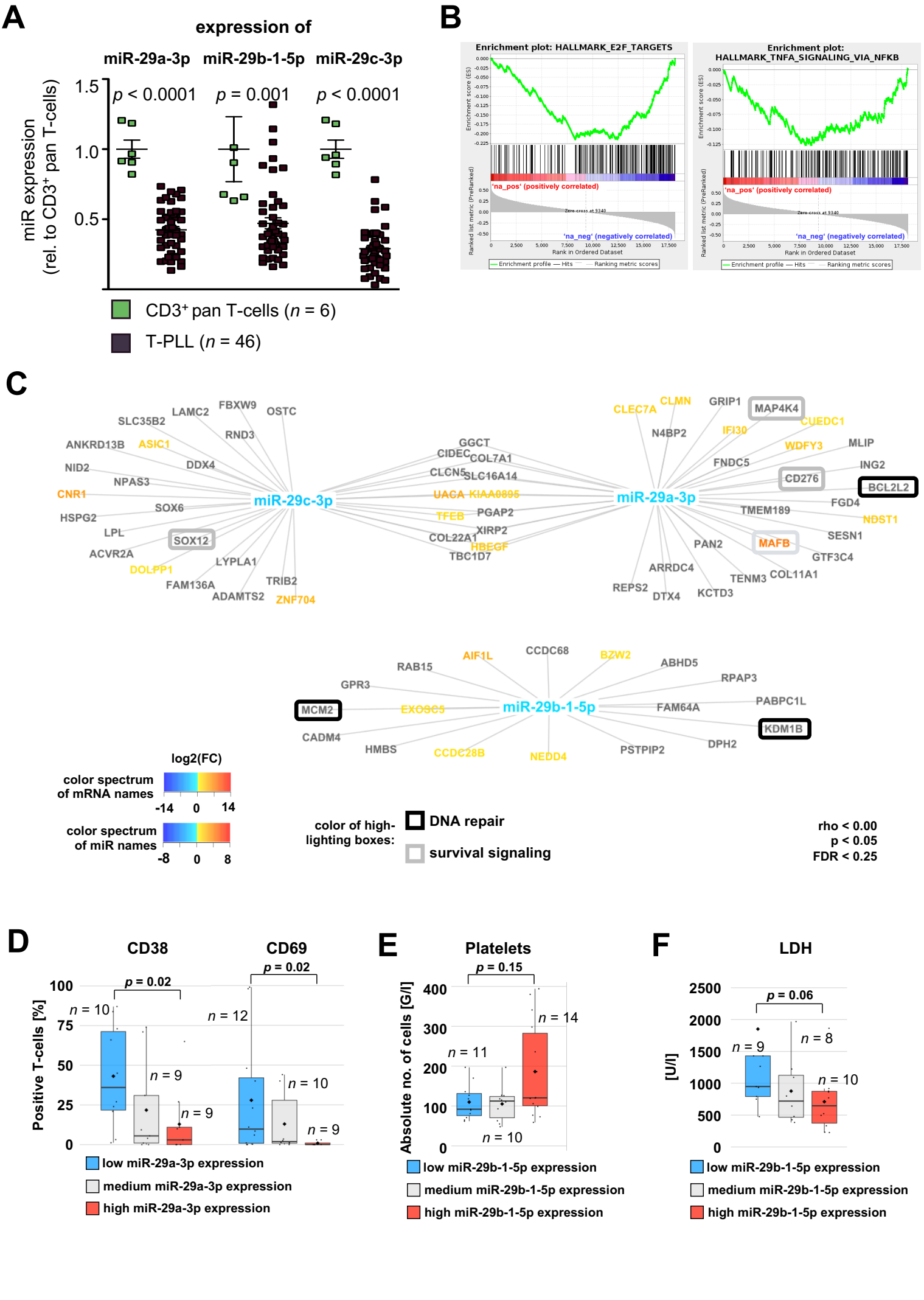
A
expression of
miR-29a-3p
miR-29b-1-5p
miR-29c-3p
p < 0.0001
p = 0.001
p < 0.0001
miR expression (rel. to CD3+ pan T-cells)
CD3+ pan T-cells (n = 6)
T-PLL (n = 46)
B
Enrichment plot: HALLMARK_E2F_TARGETS
Enrichment plot: HALLMARK_TNFA_SIGNALING_VIA_NFKB
'na_pos' (positively correlated)
'na_neg' (negatively correlated)
Rank in Ordered Dataset
Enrichment profile
Hits
Ranking metric scores
C
miR-29c-3p
miR-29a-3p
miR-29b-1-5p
log2(FC)
color spectrum of mRNA names
color spectrum of miR names
color of high-lighting boxes:
DNA repair
survival signaling
rho < 0.00
p < 0.05
FDR < 0.25
D
CD38
CD69
p = 0.02
p = 0.02
Positive T-cells [%]
low miR-29a-3p expression
medium miR-29a-3p expression
high miR-29a-3p expression
E
Platelets
p = 0.15
Absolute no. of cells [G/l]
low miR-29b-1-5p expression
medium miR-29b-1-5p expression
high miR-29b-1-5p expression
F
LDH
p = 0.06
[U/l]
low miR-29b-1-5p expression
medium miR-29b-1-5p expression
high miR-29b-1-5p expression

Figure S11

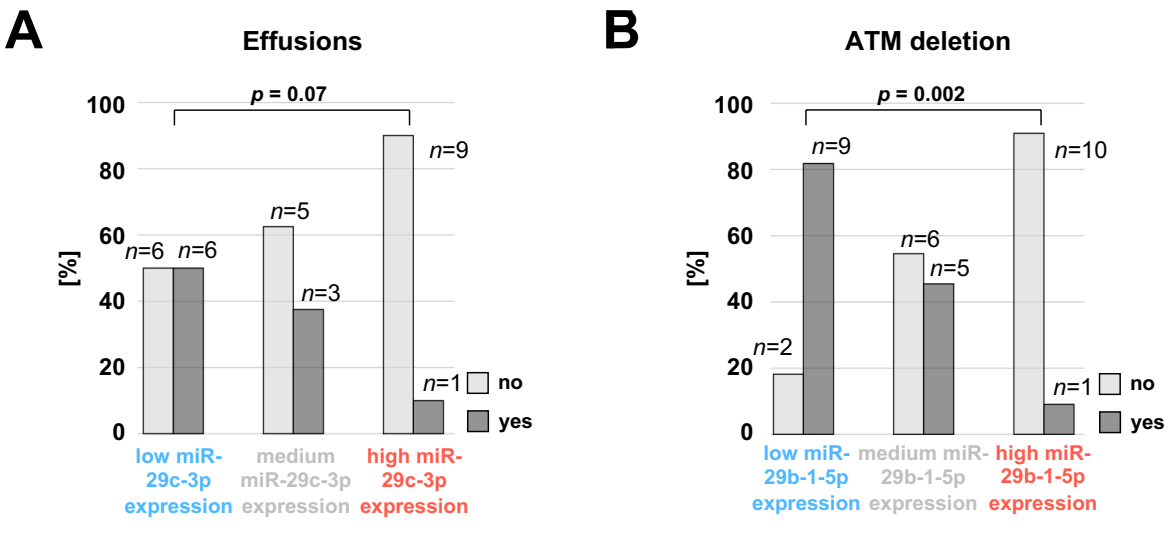
A
Effusions
p = 0.07
100
80
60
40
20
0
[%]
n=6
n=6
n=5
n=3
n=9
n=1
no
yes
low miR-29c-3p expression
medium miR-29c-3p expression
high miR-29c-3p expression
B
ATM deletion
p = 0.002
n=2
n=9
n=6
n=5
n=10
n=1
low miR-29b-1-5p expression
medium miR-29b-1-5p expression
high miR-29b-1-5p expression

Supplementary Table 1: Differentially expression of miRs comparing T-PLL cases (*n* = 46) to age-matched healthy-donor derived $CD3^+$ pan T-cells (*n* = 6).

Supplementary Table 2: Somatic copy number alterations of significantly deregulated miRs in T-PLL as detected by single nucleotide polymorphism arrays in an independent cohort of T-PLL patients.

Supplementary Table 3: Associations of immunophenotypic, cytogenetic, and clinical data with two distinct T-PLL subgroups, as revealed by unsupervised hierarchical clustering analysis of miR expression.

Supplementary Table 4: Differentially expressed mRNAs comparing two clusters of T-PLL cases (high miR-141/200c expression cluster vs. low miR-141/200c expression cluster) defined by small-RNA sequencing.

Supplementary Table 5: Differentially expressed mRNAs comparing T-PLL cases (*n* = 48) to age-matched healthy-donor derived $CD3^+$ pan T-cells (*n* = 6).

Supplementary Table 6: GSEA (*HALLMARK*) of differentially expressed mRNAs comparing T-PLL cases (n = 48) to age-matched healthy-donor derived $CD3^+$ pan T-cells (*n* = 6).

Supplementary Table 7: Differentially expressed mRNAs comparing healthy-donor derived T-cells: unstimulated control vs. TCR activated condition (*n* = 4).

Supplementary Table 8: Associations of miR-223-3p expression with immunophenotypic, cytogenetic, and clinical data (lower tertile vs. upper tertile of miR-223-3p expression).

Supplementary Table 9: Associations of miR-200c and miR-141 expression with immunophenotypic, cytogenetic, and clinical data (lower tertile vs. upper tertile of the expression of the respective miR).

Supplementary Table 10: Associations of miR-21-3p and miR-21-5p expression with immunophenotypic, cytogenetic, and clinical data (groups were divided by mean miR-21 expression).

Supplementary Table 11: Associations of miR-29c-3p, miR-29b-1-5p, and miR-29c-3p expression with immunophenotypic, cytogenetic, and clinical data (groups were divided be median miR-29 expression).

Supplementary Table 12: Associations of miR expression levels with overall survival for all miRs detectable in at least 80% of samples (*n* = 37), comparing T-PLL patients with highest expression levels (upper tertile) to those with lowest expression of the respective miR (lower tertile).

Supplementary Table 13: Associations of the miROS-T-PLL score and its miRs with incidences of genomic alterations previously described in T-PLL.

Supplementary Table 14: Associations of the miROS-T-PLL survival score with clinical, immunophenotypic and cytogenetic data (miROS-T-PLL <2 vs ≥ 2 points).